MATERIALS AND METHODS

Experimental Models and Mice

ChAT-IRES-Cre (*Chat*$^{tm2(cre)Lowl}$), ROSA-tdTomato (B6.Cg-*Gt(ROSA)26Sor*$^{tm9(CAG-tdTomato)Hze}$/J**)** and C57BL/6N-Cysltr1tm1^{Ykn}/J mice were purchased from Jackson Laboratories *(Bar Harbor, ME).* C57BL/6 mice bred in-house (originally from Charles River Laboratories, Wilmington, MA). *Ltc4s*$^{-/-}$ mice were generated on a 129Sv background and backcrossed for 15 generations onto the C57BL/6 background (*76*). $CysLT_2$- (*Cysltr2*$^{-/-}$) and $CysLT_3$-receptor gene-knockout mice (*Oxgr1*$^{-/-}$ or *Cysltr3*$^{-/-}$) were generated on a C57BL/6 background as previously described (*51, 77*). *Pou2f3*$^{-/-}$ mice were generated as described previously (*78*). *Ltc4s*$^{fl/fl}$ mice were provided by Dr. J. Boyce and generated by Ingenious targeting laboratory (Ronkonkoma, NY). B6. *Ltc4s*$^{fl/fl}$ mice with loxP sites flanking the 1st exon of *Ltc4s* were generated by homologous gene targeting in C57BL/6 embryonic stem cells. Targeted iTL BF1 (C57BL/6 FLP) embryonic stem cells were microinjected into Balb/c blastocysts. Resulting chimeras with a high percentage black coat color were mated to C57BL/6 WT mice to generate Germline Neo Deleted mice. Homozygous *Ltc4s*$^{fl/fl}$ mice were then crossed with *Chat*^{Cre} mice to generate double heterozygous mice (*Chat*$^{Cre+}$*Ltc4s*^{fl}), which were further mated with *Ltc4s* $^{fl/fl}$ mice to generate two genotypes of mice: *Ltc4s*$^{fl/fl}$ and *Chat*$^{Cre+}$*Ltc4s*$^{fl/fl}$ and used as littermate controls of each other. *Chat*$^{Cre+}$*Ltc4s*$^{fl/fl}$ were also mated to *ROSA*^{tm9tdTomato} mice to generate *Chat*$^{Cre+\ -}$*tdTomato*$^{+\ -}$ *and Chat*$^{Cre+\ -}$*tdTomato*$^{+\ -}$*Ltc4s*$^{fl/fl}$ mice.

All animals were maintained in a specific pathogen-free facility at the Brigham and Women's Hospital; litters were weaned between 19-28 days old. All experiments were performed during the day. Pooled results include both male and female mice.

Aeroallergen, cytokine and lipid mediator challenge protocols

Mice were anesthetized with an intraperitoneal injection of ketamine (10 mg/kg) and xylazine (20 mg/kg) for full sedation and received a single intranasal (i.n.) application of pharmacologic agonists or allergen dissolved in 20 µl PBS. IL-25 for intranasal challenges was dissolved in 4 nM hydrochloric acid and diluted with PBS to a final concentration of 100-500 ng/20 µl. LTC_4 was stored in ethanol; the ethanol was evaporated and LTC_4 was reconstituted in PBS for immediate application

For allergen challenge experiments, mice were given a single intranasal inhalation of 30 µg of *Alternaria alternata* (Greer) culture filtrate in 20 µl of PBS. Mice were euthanized with ketamine overdose at 1 hour for nasal lavage, at 24 hours for BAL or mediastinal lymph node digestion and at 72 hours for lung and tracheal harvesting (**Fig. 5A, 6A**).

For low-dose IL-25 and LTC_4 + IL-25 synergy experiments, mice were given three daily intranasal inhalations of 1.6 nmol of LTC_4, or 100 ng IL-25, or combination of 100 ng IL-25 and 1.6 nmol of LTC_4 in 20

µl of PBS (**Fig. 1A**). To determine if other lipid mediators cooperate with IL-25, mice were given either 2 nmol LTD_4 or 2.3 nmol LTE_4, or a combination of indicated doses of LTD_4 or LTE_4 with 100 ng IL-25.

In another set of experiments, mice were given 100, 200 or 500 ng IL-25 intranasally (**Fig. S1A**). Tissues were harvested 48 hours after the last intranasal administration.

For IL-13-induced tuft cell proliferation in the trachea, mice were given a single 5 µg of mouse IL-13 (Biolegend) in 100 µl of PBS intraperitoneally and the trachea was harvested on day 5 after the cytokine injection (**Fig. S2H**, **I**).

BAL for assessment of inflammation was collected by repetitive (n=3) instillation of 0.75 ml of PBS with 1 mM EDTA and aspiration of the fluid from the lungs through a tracheal opening. The BAL fluid was centrifuged at 500*g* for 5 min and the supernatant was discarded. Cell pellets were resuspended in 0.2 ml of PBS, and the total cells were counted manually under a microscope with a hemocytometer. For the differential cell counts of macrophages, neutrophils, and eosinophils, the BAL cells were cytospun onto fresh labeled glass slides at 500 rpm for 5 min. Air-dried slides were then stained using Diff-Quik stain kit. Cell types in a total of 400 cells were identified by morphologic criteria (*34*) and differential cell counts were performed under microscope (**Fig. 6B, Fig. S9A**).

For nasal lavage, mice were euthanized 1 hour after the intranasal challenge, and the nose was lavaged through a small incision in the trachea using 300 µl of PBS. The nasal lavage fluid proteins were precipitated with ice cold acetone and after high-speed centrifugation, the supernatant was used for CysLT and PGD_2 measurements (**Fig. 3G**).

Single cell preparations for evaluation of inflammation

For evaluation of lung inflammation, lungs were flushed with 10 ml of cold HBSS until they appeared white in color. The right lobe was removed, physically dissociated with a gentle MACS Dissociator in 10 ml of RPMI 1640 containing 10% FBS, followed by digestion with collagenase IV (500 U/ml), dispase (6.6 U/ml) and DNase I (20 µg/mL) in RPMI 1640 with 5% FCS at 37°C for 30 min with agitation at 200 rpm. The digestion was terminated by adding 10 ml of cold RPMI 1640 with 10% FBS. Cell suspensions were washed with FACS buffer and prepared for analysis by FACS.

To identify lung ILC2s among $CD45^+$ cells, lineage-positive cells were excluded using monoclonal antibodies against CD19, CD8, GR1, Fcεr1, NK1.1, CD11c, CD11b, TCRβ, TCRγδ, TER119 and CD4. ILC2 cells were identified as lin^- $Thy1.2^+$ cells with low forward and side scatter (**Fig. S1D**). Lung DCs were defined as $CD45^+$ $SiglecF^-CD11c^+MHCII^+$ cells and further differentiated based on their expression of CD301b and CD11b (*6*). Macrophages were identified as $CD45^+$ $SiglecF^+CD11b^-$ $CD11c^+$ cells, and eosinophils as $CD45^+$ $SiglecF^+CD11b^+$ $CD11c^-SSC^{high}$ after excluding B220 cells (*13*). Neutrophils were identified as $CD11b^+FSC^{low}SSC^{interm}$ cells after excluding for B220, CD8, Siglec F, CD11c, MHCII.

Ki-67 staining of the single-cell lung suspension was performed using True-Nuclear™ Transcription Factor Buffer Set (Biolegend). Surface staining of the single cells was followed by fixation with 1.4 ml of fixative from the indicated set for 1 hour, and further permeabilization with the buffer from the same set according to manufacturer's protocol. The samples were then stained with intracellular rat anti-Ki67 antibody (Invitrogen, clone SolA15) or isotype for 45-50 minutes (**Fig. 1F**, **G, S1D, F**, **G**).

For intracellular cytokine staining experiments, single-cell suspensions from the whole left lung were incubated at 37°C for 4 h in R10 media (RPMI medium 1640 containing 10% (vol/vol) FBS, 2 mM L-glutamine, 0.1 mM nonessential amino acids, penicillin (100 units/ml), streptomycin (100 µg/ml)), supplemented with 1 µl/ml of Golgi-Plug Protein Transport Inhibitor (BD Biosciences), followed by 15 min incubation with 50 µg/ml DNase I. The harvested cells were then spun at 500 × g for 10 min at 4°C and stained for extracellular markers. The samples were further washed with FACS buffer and fixed for 20 min at room temperature. The cell suspensions were permeabilized using Intracellular Staining Permeabilization Wash Buffer (Biolegend) and stained with either a mixture of PE-conjugated cytokines IL-4, IL-5, IL-13 or a PE-conjugated IgG1 isotype for 30 min (**Fig. 1H**, **I, S2A**, **B**).

To isolate immune cells from lymph nodes, the lung draining mediastinal lymph nodes were harvarested and digested in PBS solution containing collagenase IV (100 U/ml) and DNase I (20 µg/ml) for 30 mins at 37 °C. The cell suspension was stained with antibodies against CD4, CD8, B220, MHCII, CD11c, CD11b for FACS. T cells were identified as $CD8^+$ and $CD4^+$ and B cells were distinguished based on their expression of B220 while DCs were identified based on MHCII and CD11c expression (**Fig. 6C, E, S9B**, **C**).

Cytokine detection in the whole lung

For protein extraction, the frozen lobes of the right lungs were mechanically homogenized in 300 µl of T-PER protein extraction buffer supplemented with appropriate amount of protease inhibitor cocktail (cOmplete™, Mini Protease Inhibitor Cocktail, Sigma Aldrich; 10 ml T-Per buffer/1 tablet). The suspensions were spun, and the supernatants were collected. The protein concentration was measured with commercially available bicinchonic acid (BCA) protein assay kit (Thermo Fisher Scientific) according to manufacturer's instructions.

The cytokine concentrations were measured with LEGENDplex T-helper Cytokine Panel (Biolegend) in V-bottom plates, following the manufacturer's instructions. In brief, supernatants were incubated for 2 hours with fluorescence-encoded beads, differentiated by size and internal fluorescence intensities to detect 12 cytokines. The cytokine panel included IFN-γ, IL-5, TNF-α , IL-2, IL-6, IL-4, IL-10, IL-9, IL-17A, IL-17F, IL-22, IL-13 After washing, a biotinylated detection antibody cocktail was added, followed by incubation with streptavidin-phycoerythrin. Fluorescent signal intensities were then measured on 5-Laser BD FACSAria Fusion (**Fig. 2G, S2C-E**).

Single cell preparations for *ex vivo* stimulation and RNA sequencing

For single-cell preparations of the nasal mucosa, mice were euthanized and the snout was isolated and the nasal mucosa was exposed after the nasal bone was removed (*73*). The snout was incubated in pre-warmed PBS solution with dispase (16 U/ml) and deoxyribonuclease I (DNase I; 20 μg/ml) for 30 to 40 min at room temperature on a rotating shaker at 220 rpm. Dispase activity was reduced with Dulbecco's modified Eagle's medium (DMEM) and 5% fetal bovine serum (FBS) and the nasal mucosa was separated mechanically. The separated nasal mucosa was incubated in Tyrode's Solution with bicarbonate, HEPES, 0.25% BSA, without Ca^{2+}, with added 31 U/ml of papain, 25 mg/ml L-cysteine and 20 μg/ml DNAse I for 40 min at 37 °C on a rotating shaker. Papain digestion was terminated with Tyrode's Solution with HEPES and Ca^{2+} and with 2 μl/ml leupeptin (5 mg/ml). The digested tissue was vortexed for 20-30 sec, triturated thoroughly with an 18-gauge needle followed by a 21-gauge needle, passed through a 100 μm filter, and washed with FACS buffer (based on Hank's Balanced Salt Solution (HBSS) without Ca^{2+}, with added 2% FBS and 2 mM EDTA) (*15, 73*).
The resultant nasal single cell suspensions were first incubated with CD16/32 to inhibit non-specific binding for at least 30 min. The nasal epithelial cells were stained using monoclonal antibodies against CD45 and EpCAM for 40 min, followed by dead cell exclusion with propidium iodide before FACS sorting. All samples were FSC-A/SSC-A gated to exclude debris, SSC-H/SSC-W and FSC-H/SSC-W gated to select single cells. Epithelial cells from *Chat*^{Cre}*tdTomato* and *Chat*^{Cre}*tdTomatoLtc4s*$^{fl/fl}$ mice were collected based on the low/negative expression of CD45 and EpCAM expression. Tuft cells were defined as EpCAM^{high}Tomato^{+} and epithelial cells as EpCAM^{high}Tomato^{-} (**Fig. S4B**). Epithelial cells from *Ltc4s*$^{fl/fl}$ and *Chat*^{Cre}*Ltc4s*$^{fl/fl}$ mice were collected based on their expression of CD45 and three populations of cells were submitted for RNAseq: EpCAM^{high}CD45^{low}FSC^{low}SSC^{low}, EpCAM^{high}CD45^{neg}FSC^{low}SSC^{low}, and EpCAM^{int}CD45^{neg}SSC^{low} epithelial cells (**Fig. S4D**). Cells were sorted into DMEM-based epithelial cell proliferation media for *ex vivo* stimulation or TCL buffer (Qiagen) supplemented with 1% 2-mercaptoethanol for RNA sequencing.

To isolate nasal hematopoietic cells for RNAseq, the freshly isolated nasal mucosa was enzymatically dissociated with a PBS-based solution containing collagenase IV (650 U/ml), dispase (16 U/ml), and DNase I for 30 mins at 37°C on a rotating shaker. The digestion was terminated by addition of 1 ml of cold DMEM with 5% FBS. For RNA sequencing, DCs were defined as CD45^{+}CD11b^{+}SiglecF^{-}CD11c^{+}MHCII^{+} cells, and macrophages were identified as CD45^{+}CD11b^{+}SiglecF^{+}CD11c^{+} cells after excluding CD19^{+} and TCRβ^{+} cells. (**Fig. S5B**). Cell were sorted into 10 μl of TCL buffer +1% BME for RNA sequencing.

All FACS sorting was performed at the Brigham and Women's Center for Cellular Profiling using a 4-Laser BD FACSAria Fusion Cell Sorter.

***Ex vivo* stimulation of tuft cells, macrophages, and eosinophils**

For *ex vivo* assays, EpCAM^{high}CD45^{low}FSC^{low}SSC^{low} cells from *Chat^{Cre}, Ltc4s$^{fl/fl}$* and *Chat^{Cre}Ltc4s$^{fl/fl}$* mice were sorted into DMEM-based epithelial cell proliferation media, which includes DMEM/F-12, 5% Nu-Serum, 100 μg/ml Penicillin-Streptomycin (Gibco) and 0.25 μg/ml Amphotericin B. The cells were plated into 96-well culture plates at a concentration of 400,000 cells/ml in 200 μL of media per well for tuft cells and 1.2x10^6-2.3x10^{6}cells/ml in 200 μL for CD45$^+$ cells. The cells were rested overnight and stimulated with 1 mM A23187 or 0.5 mM ATPγS in 50 μl of HBSS with Ca^{2+} and Mg^{2+} for 30 min. After stimulation, the plate was centrifuged at 350 × g for 5 min at 4 °C, and the supernatants were assessed for eicosanoids.

For *ex vivo* stimulation of nasal hematopoietic cells, the nasal mucosa was processed in parallel with tuft cell isolation with dispase and papain solutions (as described above) and the single cell suspension was stained with antibodies to mark epithelial cells and macrophages. The isolated CD45$^+$ cells and CD45$^+$CD11b$^+$SiglecF$^+$CD11c$^+$ CD19$^-$TCRβ$^-$ nasal macrophages were sorted into R10 media (RPMI medium 1640 containing 10% (vol/vol) FBS, 2 mM L-glutamine, 0.1 mM nonessential amino acids, penicillin (100 units/ml), streptomycin (100 μg/ml). For *ex vivo* stimulation, the cells were plated at a concentration of 1.2x10^6-2.3x10^6 cells/ml for CD45$^+$ cells, and 66-200 x10^3 cells/ml for nasal macrophages, rested for 1-18 hours and stimulated with 1 mM A23187 for 30 min, and the supernatants were retained to assess eicosanoids.

For *ex vivo* stimulation of lung immune cells, sorted CD45$^+$ SiglecF$^+$CD11b$^-$ CD11c$^+$ lung macrophages and CD45$^+$SiglecF$^+$CD11b$^+$ CD11c$^-$SSC^{high} eosinophils were plated in R10 media at a concentration of 0.5 x10^6 cells/ml for macrophages and 0.066-1.3 x10^6 cells/ml for eosinophils. The cells were rested for 1-18 hours and stimulated with 1mM A23187. The supernatants were obtained for eicosanoid detection assays.

***In situ* Hybridization (RNAscope) and mRNA quantitation**

Tissue collection was performed under strict RNAase-free conditions. The nose and trachea were fixed with 4% PFA in DEPC-treated PBS for 12 hours. The trachea was then frozen while the nose was decalcified with DEPC-treated 14% EDTA solution for 10 days. Frozen tissue samples were sectioned to a thickness of 16 μm. For RNAscope *in situ* hybridization we used RNAscope® Fluorescent Multiplex Reagent Kit v2 (ACD, cat. No. 323120) assay following the manufacturer´s instructions. In brief, both nasal and tracheal sections were post-fixed in 4% PFA for 15 min at room temperature, treated with hydrogen peroxide for 10 min at room temperature and treated with Protease III for 10 min at 40°C before probe incubation. The probe to *Lct4s* was custom-made by ACD (Cat. No. 1092591-C1) and it targets exons 1-5 of the *Lct4s* transcript (nucleotides 98-534 of NM_008521.2). For immunohistochemistry after *in situ* hybridization, sections were rinsed in PBS after final RNAscope wash and permeabilized and blocked again with 5% NDS/0.5% Triton X-100 Sorenson´s buffer to further incubate with a mix of anti-advillin (Novus Biologicals) and anti-neurogranin (Abcam) antibodies in a dilution of 1:100 over night at 4°C. After several washes with PBS, sections were incubated with a Donkey anti rabbit antibody coupled to Alexa Fluor 647 for 2 hours and mounted in DAPI-FluoromountG.

Both WT and *Chat*^{Cre}*Lct4s*$^{fl/fl}$ tissues were treated similarly and at the same time. After RNAscope and/or immunostaining, the sections were imaged on a Leica SP8 confocal microscope. The regions in the nose epithelium were chosen based on their expression on Advillin/Neurogranin in tuft cells. On tracheal sections, random regions in the epithelium were chosen. The entire sections were imaged in consecutive z-slices separated by 1 μm using a 63x oil objective. The z stacks were then projected at maximum fluorescence intensity using Fiji/ImageJ. All quantifications were done blind to condition by assigning random numbers to each image. Only after the quantification was done, the identity of the images was revealed to assign the values to their corresponding condition. All the procedures were done under the same technical conditions and all the fluorescence parameters where kept constant between control and experimental conditions.

To quantify expression of transcripts by RNAscope, the images were applied a threshold until only puncta signal was observed. All images were treated the same way using Fiji (ImageJ). Then, the integrated density was measured as a method to quantify total mRNA puncta. In the case of nasal tissue, the signal was measured only in tuft cells, as revealed by the expression of Advillin/Neurogranin, thus the quantification represents mRNA per cell. In the case of the trachea, a random area of the tracheal epithelium, as reflected by DAPI stain, was quantified for mRNA puncta and the values represent mRNA per area of tracheal epithelium.

CysLT and PGD_2 detection

CysLT and PGD_2 detection by ELISA: CysLT and PGD_2 generation in the supernatants of tuft cells, $CD45^+$ sorted cells, and acetone-precipitated nasal lavage fluid were measured by commercially available Cysteinyl Leukotriene ELISA kit (Cayman Chemical, 500390) and Prostaglandin D_2 ELISA kit (Cayman Chemical, 512031) according to the manufacturer's instructions. The assays are based on competition between CysLTs/ PGD_2 and CysLT-acetylcholinesterase/ PGD2-acetylcholinesterase conjugate for a limited amount of CysLT/PGD_2 ELISA Monoclonal Antibody. The lower limit of detection for CysLT ELISA was 60 pg/ml and the following reported reactivity: Leukotriene C_4 (100%), Leukotriene D_4 (100%), Leukotriene E_4 (79%), 5,6-DiHETE (3.7%), Leukotriene B_4 (1.3%), 5(S)-HETE (0.04%), Arachidonic Acid (<0.01%). The lower limit of detection for PGD_2 ELISA was 19.5 pg/ml and the following reported reactivity: Prostaglandin D_2 (100%), Prostaglandin $F_{2\alpha}$ (92.4%), Prostaglandin J_2 (21.6%), Prostaglandin E_2 (2.86%), Thromboxane B_2 (2.54%), 11β-Prostaglandin $F_{2\alpha}$ (1.99%), 8-iso Prostaglandin $F_{2\alpha}$ (1.90%), Prostaglandin A_2 (0.72%), 12(S)-HHTrE (0.16%), 6-keto Prostaglandin $F_{1\alpha}$ (0.05%), (13,14-dihydro-15-keto Prostaglandin D_2) 0.02%, Arachidonic Acid (<0.01%), Leukotriene D_4 (<0.01%), tetranor-PGDM (<0.01%), tetranor-PGEM (<0.01%), tetranor-PGFM <0.01%) and tetranor-PGJM (<0.01%).

Liquid chromatography/mass spectrometry: Lipid analysis for eicosanoids (LTC_4, LTD_4, LTE_4, 5-HETE, PGD_2, $PGDE_2$, 9-HODE, 13-HODE, 9,10-EpOME and 12, 13-EpOME) was performed at the UCSD Lipidomics Core (https://www.ucsd-lipidmaps.org/home) (*74, 75*).

Targeted analysis for CysLTs was performed at the Harvard Mass Spectrometry Facility. Proteins were precipitated in samples by adding 200ul of methanol (with D4-d5 25nM as internal standard) and incubating at -80 °C for 2 hours. After centrifugation the supernatants were transferred to new microcentrifuge tubes and dried under nitrogen flow. Samples were resuspended in 20 ul of methanol:mobile phase A (see below) 1:1. A standard curve was prepared by an eight-level serial dilution (1/5, starting with a 1/40 dilution of the Cayman mix) for all compounds in methanol. 20ul of each calibration curve point was transferred to microcentrifuge tube and treated following the same protocol as the samples. Samples were analyzed on an ultimate 3000 LC coupled with a Q-exactive plus mass spectrometer (ThermoFisher). Ten microliters of samples were injected on a Kinetex C18 column (2.6u, 150x2.1 mm, Phenomenex), maintained at 30°C. The LC mobile phases were A: 10 mM ammonium Acetate, 0.1% Formic acid in water and B: Methanol, 0.2% formic acid. The gradient was as follow: starting at 20% B for 5 min, to 100% B in 10 min, followed by 10 min at 100%-, and 5-min re-equilibration at 20% B. the flow rate was maintained at 0.15 ml/min. The mass spec was set to positive polarity, with a resolution of 70000 and scanning mz 200 to 900. Compounds were quantified by integrating the area under the peaks of the compounds (extracted accurate mass at 5ppm, retention time confirmed by the authentic standards) and using the ratio with the IS to calculate the absolute concentration, using the calibration curve.

Histochemistry, immunofluorescence and quantitative assessment of goblet cell and tuft cell numbers
Assessment of goblet cell numbers. For histochemical evaluation, the left lung was embedded in glycolmethacrylate. Tissue sections, 2.5 μm thick, were assessed by PAS for quantitation of mucin-containing goblet cells and by Congo red reactivity for quantitation of eosinophil recruitment. Slides were counterstained with hematoxylin for general morphologic examination. All histologic assessments were done in a blinded fashion by a single investigator. The number of PAS-reactive cells for each animal was enumerated from 3-6 10-20x digital photographs spanning 2-13 mm basement membrane over the 4 coronal sections. This area was divided by the length of basement membrane to define the average thickness of the submucosal space.
Confocal microscopy of whole tracheal mounts. The harvested tracheas were fixed with 4% PFA, washed with PBS and permeabilized in a PBS-based blocking buffer containing 0.1% Triton X-100, 0.1% saponin, 3% bovine serum albumin, and 3% normal donkey serum for at least 3 hours. The tracheas were further incubated with primary rabbit anti-DCLK1 antibody added to the permeabilizing solution at 4°C for 48 to 72 hours. The samples were then washed with PBS containing 0.1% Triton X-100 for 3 hours and transferred to PBS containing donkey anti-rabbit secondary antibody, Alexa Fluor Plus 594 and Hoechst 33342 for nuclear stain. Tracheas were longitudinally split into two halves and embedded with the epithelial surface facing upward using a glycerol-based cover slipping solution. Images were acquired at the Brigham and Women's Hospital Confocal Microscopy Core Facility using the Zeiss LSM 800 with Airyscan confocal system on a Zeiss Axio Observer Z1 inverted microscope with 10× Zeiss [0.30 numerical aperture (NA)], 20× Zeiss (0.8 NA), and a

63× Zeiss oil (1.4 NA) objectives.

Histological quantification of tuft and goblet cells. The number of tuft cells for each trachea was enumerated from 6 to 8 photographs corresponding to 0.6-1 mm^2 taken from the same areas of each trachea starting at the distal end in proximity to the carina. The total number of DCLK1 immunoreactive cells (ranging from 131 to 205 tuft cells in unchallenged mice to 144 to 296 tuft cells in challenged mice) was divided by the area captured in the focal plane to define the number of $DCLK1^+$ cells per square millimeter. DCLK1 immuno-reactive cells and focal plane area were evaluated using ImageJ (National Institutes of Health, Bethesda, MD). Separate images were collected for each fluorochrome and overlaid to obtain a multicolor image.

To quantitate goblet cells, the number of PAS-reactive cells for each animal was enumerated from 3-6 10-20x digital photographs spanning 2-13 mm basement membrane over the 4 coronal sections. This area was divided by the length of basement membrane to define the average thickness of the submucosal space.

Low input RNA sequencing.

Preprocessing: Paired-end reads were mapped to the UCSC mm10 mouse transcriptome using Bowtie57 with parameters '-q–phred33-quals -n 1 -e 99999999 -l 25 -I 1 -X 2000 -a -m 15 -S -p 6', which allows alignment of sequences with one mismatch. For each sample, we determined the number of genes for which at least one read was mapped, and then excluded all samples with fewer than 10,000 detected genes. Only one sample was excluded in this way. Variable genes were selected using logistic regression fit to fraction of samples in which each transcript was detected, using the log of total transcripts for each gene as a predictor. Outliers from this curve are genes that are expressed in a lower fraction of samples than would be expected given the total number of reads mapping to that gene, that is, treatment condition or state-specific genes. We used a threshold of deviance <−0.2, producing a set of 2307 variable genes. We restricted the expression matrix to this subset of variable genes and took the variance stabilizing transformation log2(TPM +1) to generate the digital gene expression (DGE) matrix that was used for all downstream analysis. We performed dimensionality reduction on the DGE matrix using PCA. Values were centered and scaled before input to PCA, which was implemented using the R function 'prcomp' from the 'stats' package. The data were visualized in Fig. 3 using the first two principal components, which accounted for 29% and 10% of the variance respectively.

Comparison to known tuft cell signature: Tuft cell marker genes were derived from the 'consensus' signature defined with single-cell RNA sequencing (*9*). Heatmaps were generated using the 'pheatmap' R package.

Correlation of nasal epithelial groups: Pairwise Pearson correlations between all samples were calculated using the R function 'cor' from the 'stats' package (**Fig. S3D**). To identify the similarity between the putative prospectively isolated tuft cells ($Ltc4s^{fl/fl}$ $EpCAM^{high}$ $CD45^{low}$), the mean expression of each gene across the $Ltc4s^{fl/fl}$ $EpCAM^{high}$ $CD45^{low}$ tuft cell-enriched samples and used this as a reference signature to calculate

Pearson correlations with other samples. We visualized the correlation of each sample to the *Ltc4s*$^{fl/fl}$ EpCAM^{high} CD45^{low} consensus signature, grouped by sample population, and ranked these by their mean correlation.

***Ltc4s* expression in neurons:** Expression data for mouse neuronal populations was downloaded from the Mouse Brain Atlas (http://mousebrain.org/downloads.html) and visualized using the 'ggplot2' package in R.

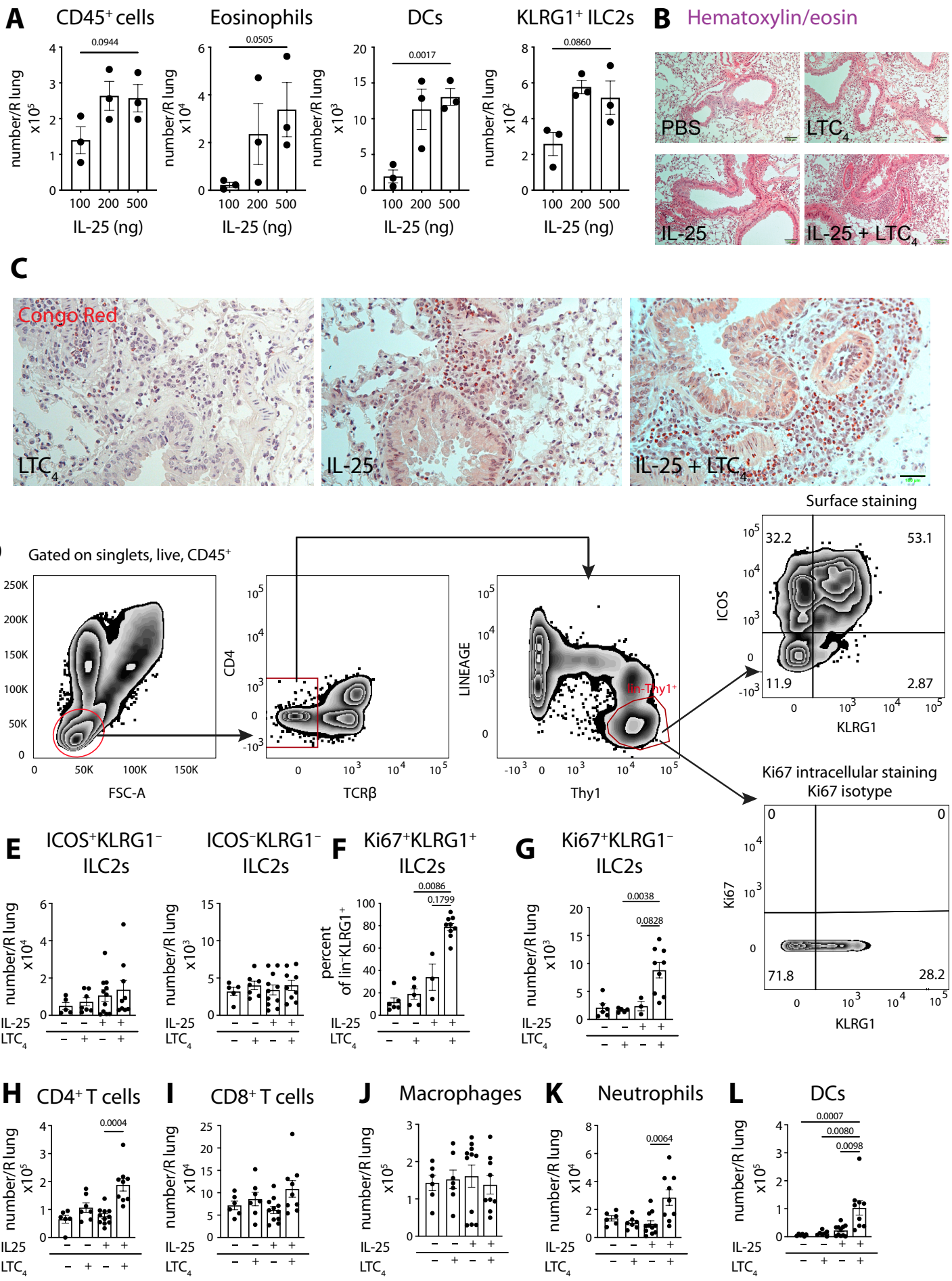
A
CD45+ cells
Eosinophils
DCs
KLRG1+ ILC2s
number/R lung
IL-25 (ng)
0.0944
0.0505
0.0017
0.0860
B
Hematoxylin/eosin
PBS
LTC4
IL-25
IL-25 + LTC4
C
Congo Red
LTC4
IL-25
IL-25 + LTC4
D
Gated on singlets, live, CD45+
SSC-A
FSC-A
CD4
TCRβ
LINEAGE
Thy1
lin-Thy1+
Surface staining
ICOS
KLRG1
32.2
53.1
11.9
2.87
Ki67 intracellular staining
Ki67 isotype
Ki67
71.8
28.2
E
ICOS+KLRG1− ILC2s
ICOS−KLRG1− ILC2s
F
Ki67+KLRG1+ ILC2s
percent of lin−KLRG1+
0.0086
0.1799
G
Ki67+KLRG1− ILC2s
0.0038
0.0828
IL-25
LTC4
H
CD4+ T cells
0.0004
I
CD8+ T cells
J
Macrophages
K
Neutrophils
0.0064
L
DCs
0.0007
0.0080
0.0098

Fig. S1. LTC_4 and IL-25 synergize for airway type 2 lung inflammation.
(A) C57BL/6 were given three daily intranasal inhalations of IL-25 at three doses (100, 200, and 500 ng) and lung inflammation was assessed by FACS of the lung 48 hours after the last intranasal IL-25 administration. (**B-L**) WT mice were given three daily inhalations of LTC_4 (1.6 nmol) or IL-25 (100 ng) or a combination of LTC_4 and IL-25 and assessed 48 hours after the last dose (as in **Fig. 1A**). (**B**) Lung inflammation was visualized by Hematoxylin and Eosin stain. (**C**) Eosinophils were visualized with Congo Red stain. Scale bar indicates 100 μm. (**D**) Gating strategy for ILC2s and ILC2 proliferation by Ki67. (**E**) Counts of $ICOS^+KLRG1^-$ILC2s and $ICOS^-KLRG1^-$ILC2s in the right lung by FACS. (**F**) Frequency of $Ki67^+$ cells within the $KLRG1^+$ILC2 subset. (**G**) Number of $Ki67^+KLRG1^-$ILC2s, (**H**) number of $CD4^+$ T cells, (**I**) number of $CD8^+$ T cells, (**J**) number of macrophages, (**K**) number of neutrophils and (**L**) number DCs in the lung assessed by FACS. Data are means ± SEM pooled from 3 independent experiments, each dot is a mouse, p values indicated, Kruskal-Wallis ANOVA with Dunn's correction for multiple comparisons.

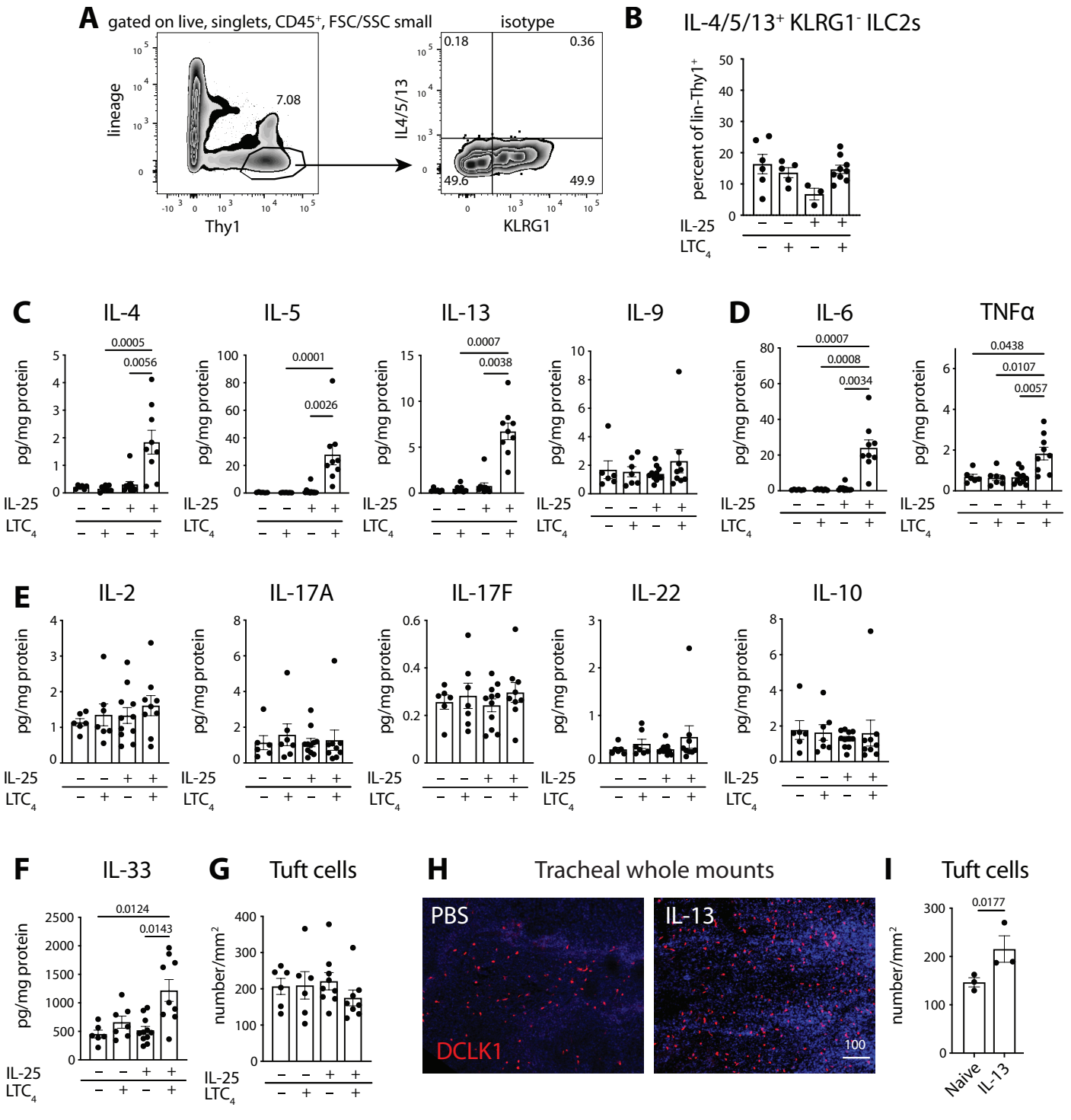
A
gated on live, singlets, CD45+, FSC/SSC small
isotype
lineage
Thy1
7.08
IL4/5/13
KLRG1
0.18
0.36
49.6
49.9
B
IL-4/5/13+ KLRG1- ILC2s
percent of lin-Thy1+
IL-25
LTC4
C
IL-4
IL-5
IL-13
IL-9
pg/mg protein
0.0005
0.0056
0.0001
0.0026
0.0007
0.0038
D
IL-6
TNFα
0.0007
0.0008
0.0034
0.0438
0.0107
0.0057
E
IL-2
IL-17A
IL-17F
IL-22
IL-10
F
IL-33
0.0124
0.0143
G
Tuft cells
number/mm2
H
Tracheal whole mounts
PBS
IL-13
DCLK1
100
I
Tuft cells
0.0177
Naive
IL-13

Fig. S2. Lung cytokine profile and tuft cell numbers after LTC_4 and IL-25 inhalation.
(**A**) Gating strategy for ILC2 cytokine production and isotype control for IL-4/5/13. (**B**) Percent of type 2 cytokine expressing $KLRG1^-$ cells expressed as percent of $Thy1^+$ ILC2 cells defined by FACS. (**C-E**) Cytokine concentration of whole lung homogenates was determined by LegendPlex ELISA and expressed as pg per mg of lung protein. (**F**) Lung IL-33 was measured in whole lung homogenates by ELISA and expressed as pg per mg protein. Data are means ± SEM pooled from 3 independent experiments, each dot is a separate mouse, p values <0.05 indicated, Kruskal-Wallis ANOVA with Dunn's correction for multiple comparisons. (**G-I**) Tuft cells ($DCLK1^+$) numbers were assessed in whole trachea mounts in mice given inhalations of IL-25 and LTC_4 (**G**) or intraperitoneal injections of IL-13 (**H**, **I**), n=3 experiment for G, n=1 experiment for **H**, **I** each dot represents a separate mouse, p value from negative binomial regression. Scale bar in μm.

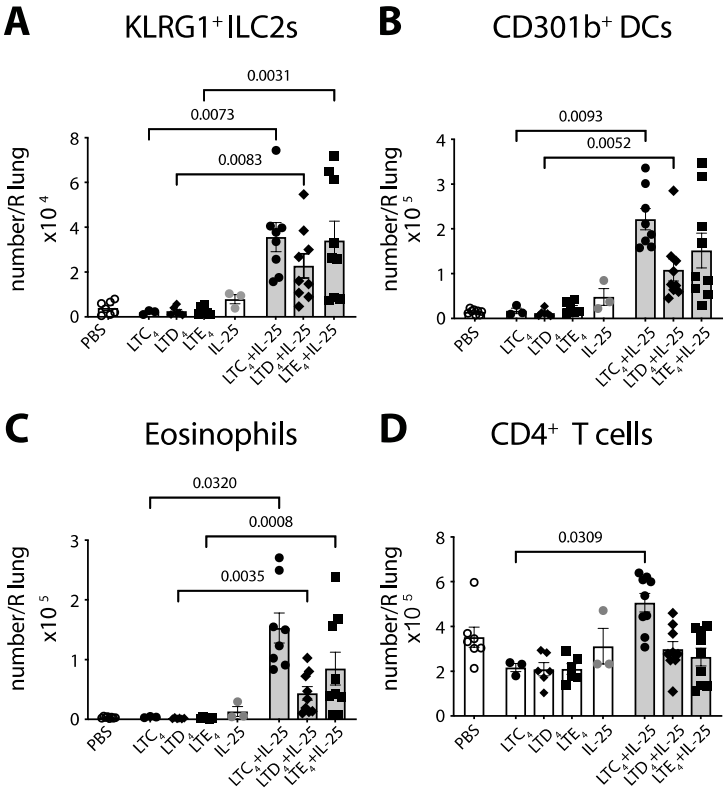
A
KLRG1+ ILC2s
number/R lung
x10 4
0.0031
0.0073
0.0083
PBS
LTC4
LTD4
LTE4
IL-25
LTC4+IL-25
LTD4+IL-25
LTE4+IL-25
B
CD301b+ DCs
number/R lung
x10 5
0.0093
0.0052
C
Eosinophils
number/R lung
x10 5
0.0320
0.0008
0.0035
D
CD4+ T cells
number/R lung
x10 5
0.0309

Fig. S3. CysLT synergy with IL-25 to promote lung inflammation *in vivo* is primarily driven by LTC_4. WT mice were given three daily inhalations of LTC_4, LTD_4 or LTE_4 alone, IL-25 (100 ng) alone or a combination of each CysLT with IL-25 and assessed 48 hours after the last dose. (**A**) Absolute counts of $KLRG1^+$ILC2s, (**B**) $CD301b^+$ DCs, (**C**) eosinophils, and (**D**) $CD4^+$ T cells in the lung was assessed by FACS. Data are means ± SEM pooled from 3 independent experiments, each dot is a separate mouse, p values <0.05 indicated, Kruskal-Wallis ANOVA with Dunn's correction for multiple comparisons.

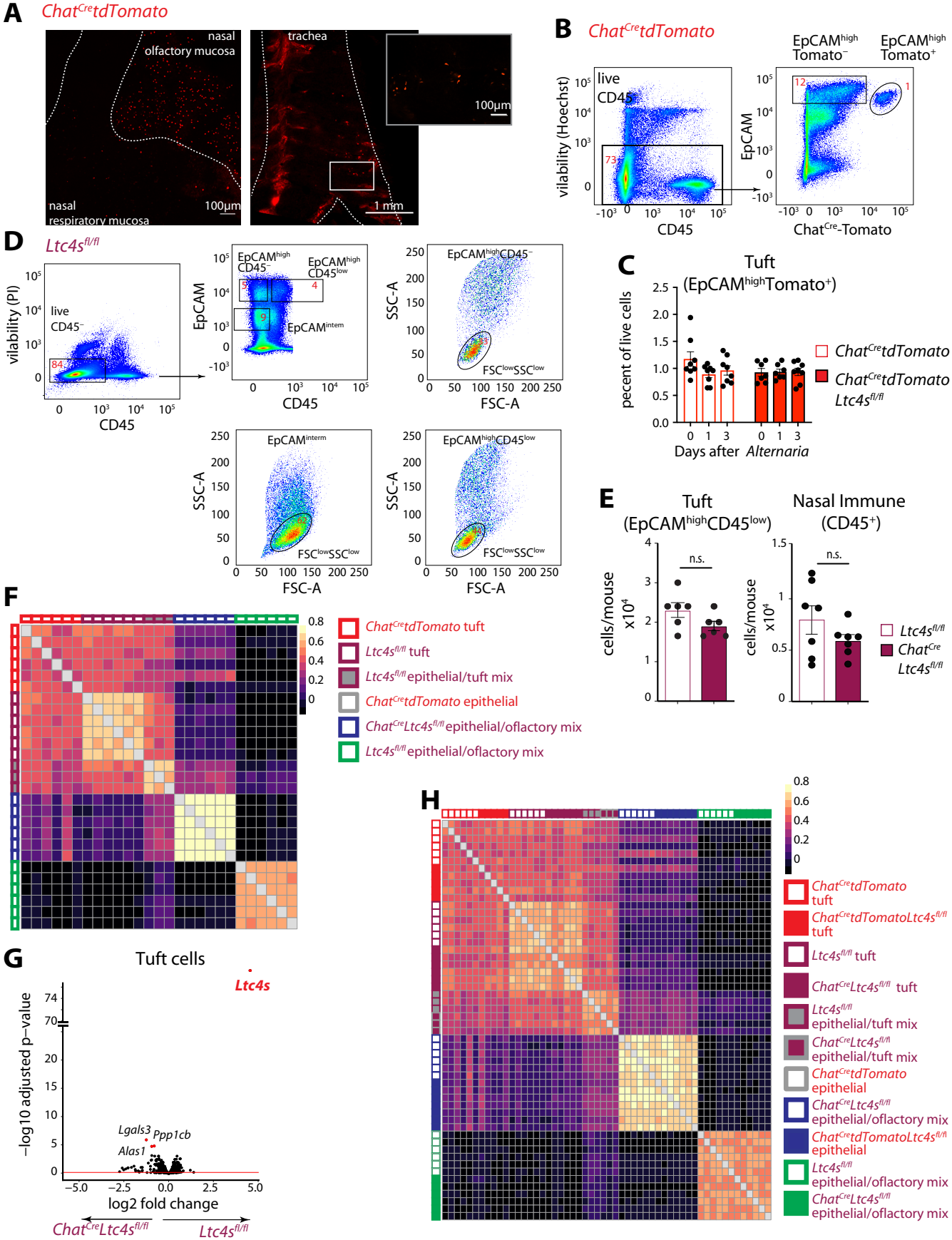
A
Chat^Cre tdTomato
nasal olfactory mucosa
100μm
nasal respiratory mucosa
100μm
trachea
100μm
1 mm
B
Chat^Cre tdTomato
live CD45+
vilability (Hoechst)
CD45
EpCAM^high Tomato^−
EpCAM^high Tomato^+
EpCAM
Chat^Cre-Tomato
D
Ltc4s^fl/fl
vilability (PI)
live CD45−
CD45
EpCAM^high CD45−
EpCAM^high CD45^low
EpCAM^interm
EpCAM
SSC-A
FSC-A
FSC^lowSSC^low
EpCAM^high CD45−
EpCAM^interm
EpCAM^high CD45^low
C
Tuft (EpCAM^high Tomato^+)
pecent of live cells
Days after Alternaria
Chat^Cre tdTomato
Chat^Cre tdTomato Ltc4s^fl/fl
E
Tuft (EpCAM^high CD45^low)
Nasal Immune (CD45^+)
cells/mouse x10^4
n.s.
Ltc4s^fl/fl
Chat^Cre Ltc4s^fl/fl
F
Chat^Cre tdTomato tuft
Ltc4s^fl/fl tuft
Ltc4s^fl/fl epithelial/tuft mix
Chat^Cre tdTomato epithelial
Chat^Cre Ltc4s^fl/fl epithelial/oflactory mix
Ltc4s^fl/fl epithelial/oflactory mix
G
Tuft cells
Ltc4s
−log10 adjusted p−value
log2 fold change
Lgals3
Ppp1cb
Alas1
Chat^Cre Ltc4s^fl/fl
Ltc4s^fl/fl
H
Chat^Cre tdTomato tuft
Chat^Cre tdTomato Ltc4s^fl/fl tuft
Ltc4s^fl/fl tuft
Chat^Cre Ltc4s^fl/fl tuft
Ltc4s^fl/fl epithelial/tuft mix
Chat^Cre Ltc4s^fl/fl epithelial/tuft mix
Chat^Cre tdTomato epithelial
Chat^Cre Ltc4s^fl/fl epithelial/oflactory mix
Chat^Cre tdTomato Ltc4s^fl/fl epithelial
Ltc4s^fl/fl epithelial/oflactory mix
Chat^Cre Ltc4s^fl/fl epithelial/oflactory mix

Fig. S4. EpCAM^{high} CD45 ^{low} cells are highly enriched for tuft cells. (**A**) Whole mount of nose with olfactory and respiratory portion (left) and whole mount of trachea (right) from a *Chat^{Cre}tdTomato* mouse. (**B**) Gating strategy for isolation of tuft cells and epithelial cells from the nasal mucosa of *Chat^{Cre}tdTomato* mice. (**C**) Comparison of the numbers and frequency of tuft cells from control *Chat^{Cre}tdTomato* mice to mice with conditional deletion of *Ltc4s (Chat^{Cre}tdTomatoLTC4s$^{fl/fl}$*. (**D**) Gating strategy for isolation of tuft cells from the nasal mucosa of *Ltc4s$^{fl/fl}$* mice. Three populations of EpCAM^{+} cells were distinguished – EpCAM^{high}CD45^{+}, EpCAM^{high}CD45^{-} and EpCAM^{interm}. (**E**) Comparison of the numbers and frequency of tuft cells and CD45^{+} cells from *Ltc4s$^{fl/fl}$* and *Chat^{Cre}Ltc4s$^{fl/fl}$* mice. (**F**) Heatmap demonstrating Pearson's correlation coefficient across expression levels of all highly variable genes (Methods) between all pairs of samples from nasal epithelial groups from *Chat^{Cre}tdTomato* and *Ltc4s$^{fl/fl}$* mice, samples are ordered by cluster assignment (color legend). (**G**) Volcano plot displaying significance (y axis, -log10(FDR)) of differential expression (x axis, log2 fold-change) in EpCAM^{high}CD45^{low} tuft cell-enriched cells between *Ltc4s$^{fl/fl}$* and *Chat^{Cre}Ltc4s$^{fl/fl}$* mice. Note split Y axis to highlight genes with low level of fold change and significance. (**H**) Heatmap demonstrating Pearson's correlation coefficient across tuft cells and epithelial cells from mice with and without conditional deletion of *Ltc4s*.

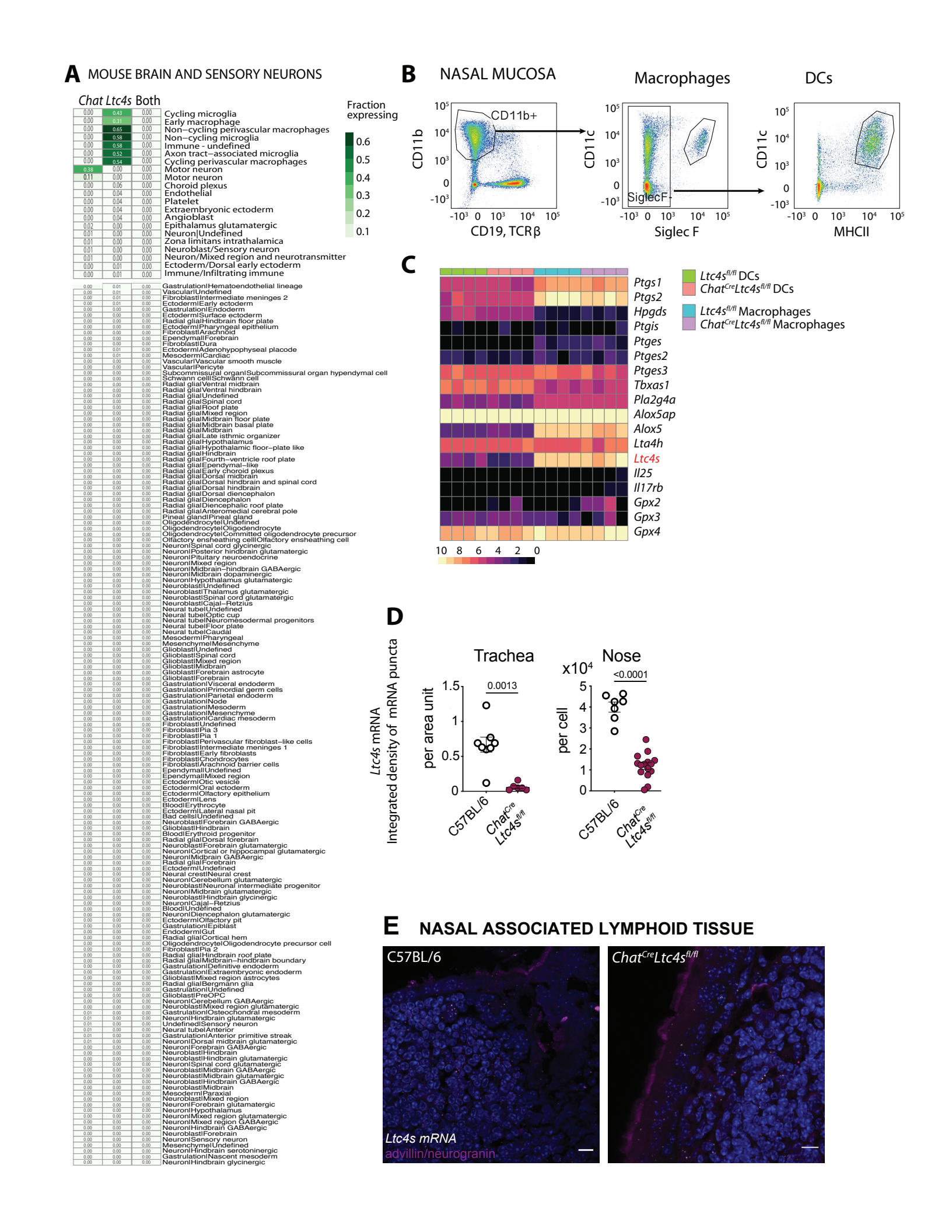
A
MOUSE BRAIN AND SENSORY NEURONS
Chat Ltc4s Both
Fraction expressing
0.6
0.5
0.4
0.3
0.2
0.1
Cycling microglia
Early macrophage
Non−cycling perivascular macrophages
Non−cycling microglia
Immune - undefined
Axon tract−associated microglia
Cycling perivascular macrophages
Motor neuron
Motor neuron
Choroid plexus
Endothelial
Platelet
Extraembryonic ectoderm
Angioblast
Epithalamus glutamatergic
Neuron|Undefined
Zona limitans intrathalamica
Neuroblast/Sensory neuron
Neuron/Mixed region and neurotransmitter
Ectoderm/Dorsal early ectoderm
Immune/Infiltrating immune
Gastrulation|Hematoendothelial lineage
Vascular|Undefined
Fibroblast|Intermediate meninges 2
Ectoderm|Early ectoderm
Gastrulation|Endoderm
Ectoderm|Surface ectoderm
Radial glial|Hindbrain floor plate
Ectoderm|Pharyngeal epithelium
Fibroblast|Arachnoid
Ependymal|Forebrain
Fibroblast|Dura
Ectoderm|Adenohypophyseal placode
Mesoderm|Cardiac
Vascular|Vascular smooth muscle
Vascular|Pericyte
Subcommissural organ|Subcommissural organ hypendymal cell
Schwann cell|Schwann cell
Radial glial|Ventral midbrain
Radial glial|Ventral hindbrain
Radial glial|Undefined
Radial glial|Spinal cord
Radial glial|Roof plate
Radial glial|Mixed region
Radial glial|Midbrain floor plate
Radial glial|Midbrain basal plate
Radial glial|Midbrain
Radial glial|Late isthmic organizer
Radial glial|Hypothalamus
Radial glial|Hypothalamic floor−plate like
Radial glial|Hindbrain
Radial glial|Fourth−ventricle roof plate
Radial glial|Ependymal−like
Radial glial|Early choroid plexus
Radial glial|Dorsal midbrain
Radial glial|Dorsal hindbrain and spinal cord
Radial glial|Dorsal hindbrain
Radial glial|Dorsal diencephalon
Radial glial|Diencephalon
Radial glial|Diencephalic roof plate
Radial glial|Anteromedial cerebral pole
Pineal gland|Pineal gland
Oligodendrocyte|Undefined
Oligodendrocyte|Oligodendrocyte
Oligodendrocyte|Committed oligodendrocyte precursor
Olfactory ensheathing cell|Olfactory ensheathing cell
Neuron|Spinal cord glycinergic
Neuron|Posterior hindbrain glutamatergic
Neuron|Pituitary neuroendocrine
Neuron|Mixed region
Neuron|Midbrain−hindbrain GABAergic
Neuron|Midbrain dopaminergic
Neuron|Hypothalamus glutamatergic
Neuroblast|Undefined
Neuroblast|Thalamus glutamatergic
Neuroblast|Spinal cord glutamatergic
Neuroblast|Cajal−Retzius
Neural tube|Undefined
Neural tube|Optic cup
Neural tube|Neuromesodermal progenitors
Neural tube|Floor plate
Neural tube|Caudal
Mesoderm|Pharyngeal
Mesenchyme|Mesenchyme
Glioblast|Undefined
Glioblast|Spinal cord
Glioblast|Mixed region
Glioblast|Midbrain
Glioblast|Forebrain astrocyte
Glioblast|Forebrain
Gastrulation|Visceral endoderm
Gastrulation|Primordial germ cells
Gastrulation|Parietal endoderm
Gastrulation|Node
Gastrulation|Mesoderm
Gastrulation|Mesenchyme
Gastrulation|Cardiac mesoderm
Fibroblast|Undefined
Fibroblast|Pia 3
Fibroblast|Pia 1
Fibroblast|Perivascular fibroblast−like cells
Fibroblast|Intermediate meninges 1
Fibroblast|Early fibroblasts
Fibroblast|Chondrocytes
Fibroblast|Arachnoid barrier cells
Ependymal|Undefined
Ependymal|Mixed region
Ectoderm|Otic vesicle
Ectoderm|Oral ectoderm
Ectoderm|Olfactory epithelium
Ectoderm|Lens
Blood|Erythrocyte
Ectoderm|Lateral nasal pit
Bad cells|Undefined
Neuroblast|Forebrain GABAergic
Glioblast|Hindbrain
Blood|Erythroid progenitor
Radial glial|Dorsal forebrain
Neuroblast|Forebrain glutamatergic
Neuron|Cortical or hippocampal glutamatergic
Neuron|Midbrain GABAergic
Radial glial|Forebrain
Ectoderm|Undefined
Neural crest|Neural crest
Neuron|Cerebellum glutamatergic
Neuroblast|Neuronal intermediate progenitor
Neuron|Midbrain glutamatergic
Neuroblast|Hindbrain glycinergic
Neuron|Cajal−Retzius
Blood|Undefined
Neuron|Diencephalon glutamatergic
Ectoderm|Olfactory pit
Gastrulation|Epiblast
Endoderm|Gut
Radial glial|Cortical hem
Oligodendrocyte|Oligodendrocyte precursor cell
Fibroblast|Pia 2
Radial glial|Hindbrain roof plate
Radial glial|Midbrain−hindbrain boundary
Gastrulation|Definitive endoderm
Gastrulation|Extraembryonic endoderm
Glioblast|Mixed region astrocytes
Radial glial|Bergmann glia
Gastrulation|Undefined
Glioblast|PreOPC
Neuron|Cerebellum GABAergic
Neuroblast|Mixed region glutamatergic
Gastrulation|Osteochondral mesoderm
Neuron|Hindbrain glutamatergic
Undefined|Sensory neuron
Neural tube|Anterior
Gastrulation|Anterior primitive streak
Neuron|Dorsal midbrain glutamatergic
Neuron|Forebrain GABAergic
Neuroblast|Hindbrain
Neuroblast|Hindbrain glutamatergic
Neuron|Spinal cord glutamatergic
Neuroblast|Midbrain GABAergic
Neuroblast|Midbrain glutamatergic
Neuroblast|Hindbrain GABAergic
Neuroblast|Midbrain
Mesoderm|Paraxial
Neuroblast|Mixed region
Neuron|Forebrain glutamatergic
Neuron|Hypothalamus
Neuron|Mixed region glutamatergic
Neuron|Mixed region GABAergic
Neuron|Hindbrain GABAergic
Neuroblast|Forebrain
Neuron|Sensory neuron
Mesenchyme|Undefined
Neuron|Hindbrain serotoninergic
Gastrulation|Nascent mesoderm
Neuron|Hindbrain glycinergic
B
NASAL MUCOSA
Macrophages
DCs
CD11b+
CD11b
CD19, TCRβ
CD11c
Siglec F
SiglecF+
CD11c
MHCII
C
Ptgs1
Ptgs2
Hpgds
Ptgis
Ptges
Ptges2
Ptges3
Tbxas1
Pla2g4a
Alox5ap
Alox5
Lta4h
Ltc4s
Il25
Il17rb
Gpx2
Gpx3
Gpx4
10 8 6 4 2 0
Ltc4s fl/fl DCs
ChatCre Ltc4s fl/fl DCs
Ltc4s fl/fl Macrophages
ChatCre Ltc4s fl/fl Macrophages
D
Ltc4s mRNA
Integrated density of mRNA puncta
Trachea
Nose
per area unit
per cell
0.0013
<0.0001
C57BL/6
ChatCre Ltc4s fl/fl
E
NASAL ASSOCIATED LYMPHOID TISSUE
C57BL/6
ChatCre Ltc4s fl/fl
Ltc4s mRNA
adyillin/neurogranin

Fig. S5. *Chat* and *Ltc4s* are not co-expressed in neurons or immune cells. (**A**) Fraction of cells expressing *Chat* (first column), *Ltc4s* (second column) and both transcripts (third column) in central and peripheral neurons and nervous system immune cells from previously published data downloaded from the Mouse Brain Atlas (*46*). (**B**) DCs and macrophages were defined within the $CD45^+$ cell subset as $CD19^-$ (B cell marker), $TCR\beta^-$ (T cell marker), $CD11b^+$, and $SiglecF^+$ for macrophages. DCs were further defined as $SiglecF^-$ $CD11c^+$ and $MHCII^+$. (**C**) Heatmap shows expression (log2(TPM+1), color bar) of genes in the 5-lipoxygenase and cyclooxygenase pathways in DCs and macrophages derived from $Ltc4s^{fl/fl}$ and $Chat^{Cre}Ltc4s^{fl/fl}$ mice. (**D**) *Ltc4s* mRNA was quantitated as the integrated density of puncta in the epithelium of the trachea (WT: 8, $Chat^{Cre}Ltc4s^{fl/fl}$: 6 images) and nose (WT: 7, $Chat^{Cre}Ltc4s^{fl/fl}$: 15 images). (**E**) *In situ* hybridization for *Ltc4s* in nasal associated lymphoid tissue (nasal submucosa) of WT and $Chat^{Cre}Ltc4s^{fl/fl}$ mice. Scale bar 100 μm.

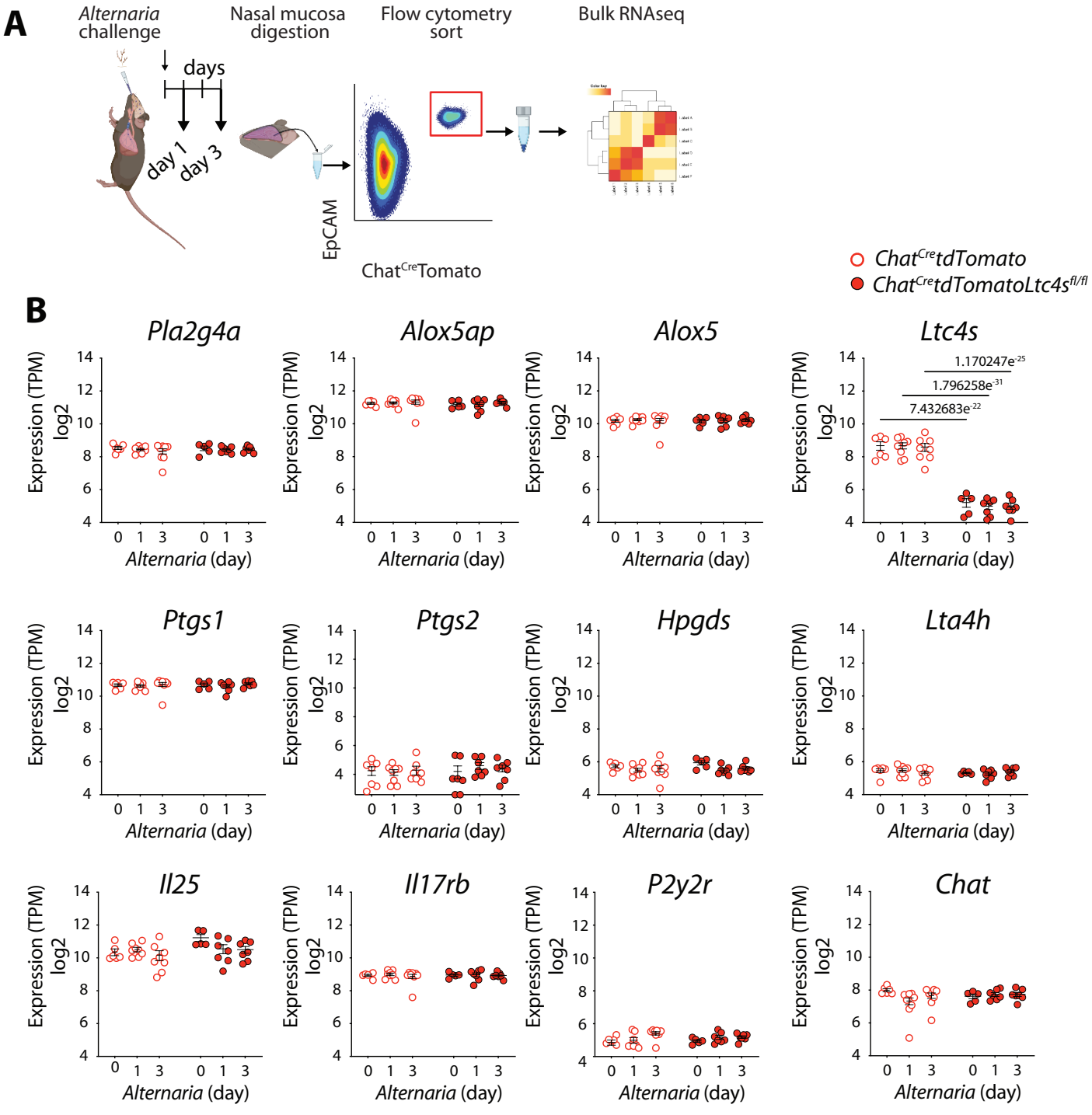
A
Alternaria challenge
Nasal mucosa digestion
Flow cytometry sort
Bulk RNAseq
days
day 1
day 3
EpCAM
ChatCreTomato
ChatCretdTomato
ChatCretdTomatoLtc4sfl/fl
B
Pla2g4a
Alox5ap
Alox5
Ltc4s
1.170247e-25
1.796258e-31
7.432683e-22
Ptgs1
Ptgs2
Hpgds
Lta4h
Il25
Il17rb
P2y2r
Chat
Expression (TPM) log2
Alternaria (day)
0 1 3 0 1 3

Fig. S6. The eicosanoid transcriptional profile of tuft cells is unaltered by *Alternaria* challenge.
(**A**) *Chat*^{Cre}*tdTomato* and *Chat*^{Cre}*tdTomatoLtc4s*$^{fl/fl}$ mice were given a single intranasal inhalation of *Alternaria* allergen and tuft cells were isolated based on their expression of EpCAM and tdTomato 39 hours or 72 hours after the challenge. (**B**) The tuft cell transcriptional profile was evaluated by bulk RNAseq. Expression level in transcripts per million (TPM) of the indicated genes. Data are means ± SEM from two independent experiments, each mouse is a separate dot. Normalization and differential expression analysis was performed by DeSeq2.

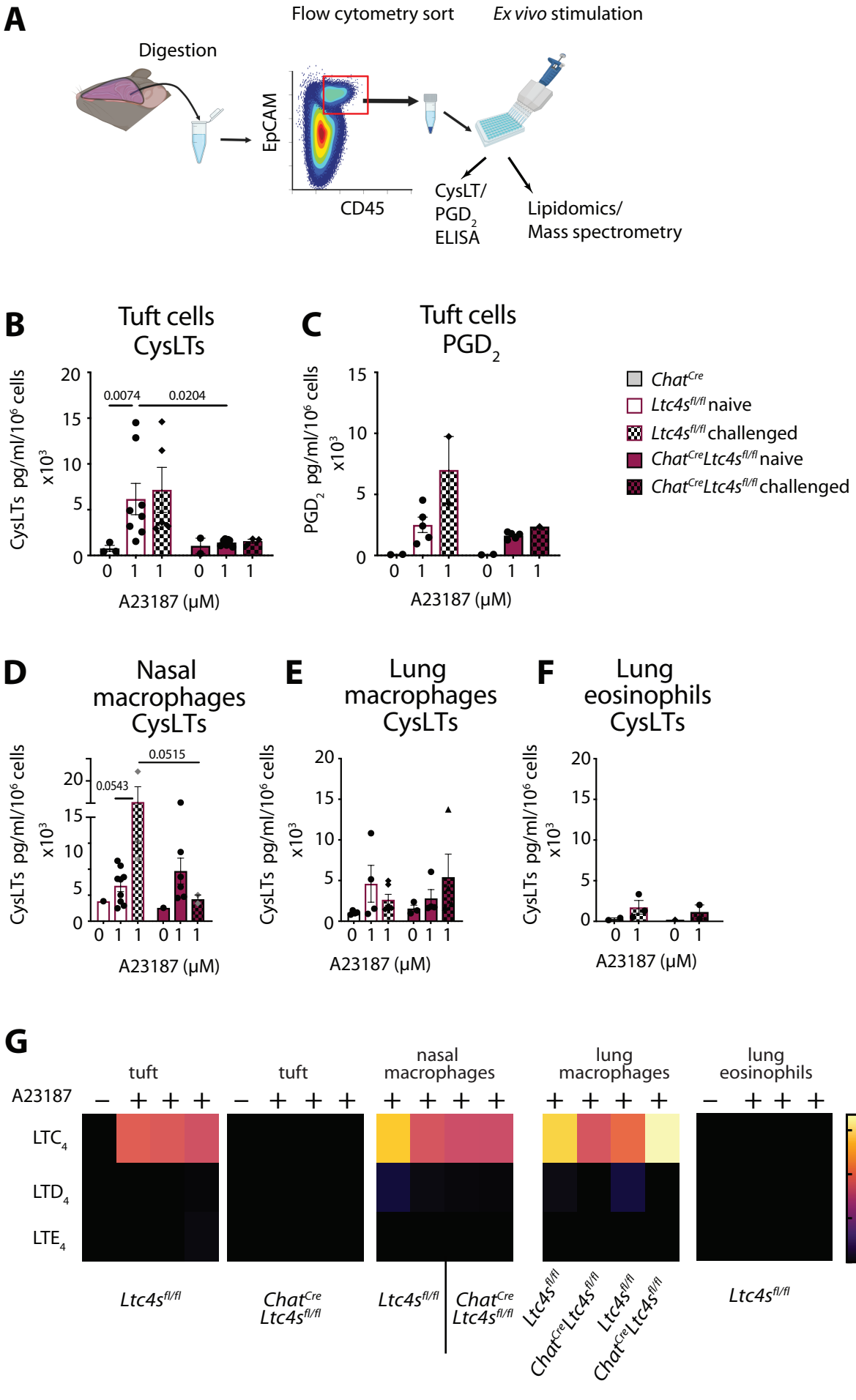
A
Digestion
Flow cytometry sort
Ex vivo stimulation
EpCAM
CD45
CysLT/
PGD2
ELISA
Lipidomics/
Mass spectrometry
B
Tuft cells
CysLTs
CysLTs pg/ml/10⁶ cells
x10³
0.0074
0.0204
A23187 (μM)
C
Tuft cells
PGD2
PGD2 pg/ml/10⁶ cells
x10³
A23187 (μM)
ChatCre
Ltc4sfl/fl naive
Ltc4sfl/fl challenged
ChatCreLtc4sfl/fl naive
ChatCreLtc4sfl/fl challenged
D
Nasal
macrophages
CysLTs
0.0543
0.0515
E
Lung
macrophages
CysLTs
F
Lung
eosinophils
CysLTs
G
tuft
tuft
nasal
macrophages
lung
macrophages
lung
eosinophils
A23187
LTC4
LTD4
LTE4
3000
2000
1000
0
Ltc4sfl/fl
ChatCre
Ltc4sfl/fl
Ltc4sfl/fl
ChatCre
Ltc4sfl/fl
Ltc4sfl/fl
ChatCreLtc4sfl/fl
Ltc4sfl/fl
ChatCreLtc4sfl/fl
Ltc4sfl/fl

Fig. S7. *Ltc4s* deletion does not alter the eicosanoid generating capacity of airway immune cells. (**A**) Tuft cells were isolated from the nasal mucosa of *Chat*^{Cre}, *Ltc4s*$^{fl/fl}$ and *Chat*^{Cre}*Ltc4s*$^{fl/fl}$ based on their expression of EpCAM and CD45. The sorted cells were rested overnight and stimulated *ex vivo* with Ca^{2+} ionophore (A23187) or ATPγS. The concentration of eicosanoids in the supernatants was measured by ELISA or lipidomics/LC-MS. Mice were evaluated both in the naïve state and 36 hours after *Alternaria* challenge (**B**) CysLTs in the supernatant of tuft cells stimulated with Ca^{2+} ionophore A23187 measured by ELISA. (**C**) PGD_2 in the supernatant of tuft cells stimulated with Ca^{2+} ionophore A23187 measured by ELISA. (**D**-**F**) CysLTs in the supernatants of nasal macrophages (D), lung macrophages (E) and lung eosinophils (F) stimulated with A23187, measured by ELISA. (**G**) Heatmap of expression (pg/ml of sample) of CysLTs assessed by liquid chromatography/mass spectrometry. Tuft cells, nasal and lung macrophages and eosinophils were sorted from naïve and *Alternaria* challenged mice (eosinophils). Cells were stimulated with HBSS or A23187 and the supernatants were assessed after 30 min. Data is expressed as pg/ml.

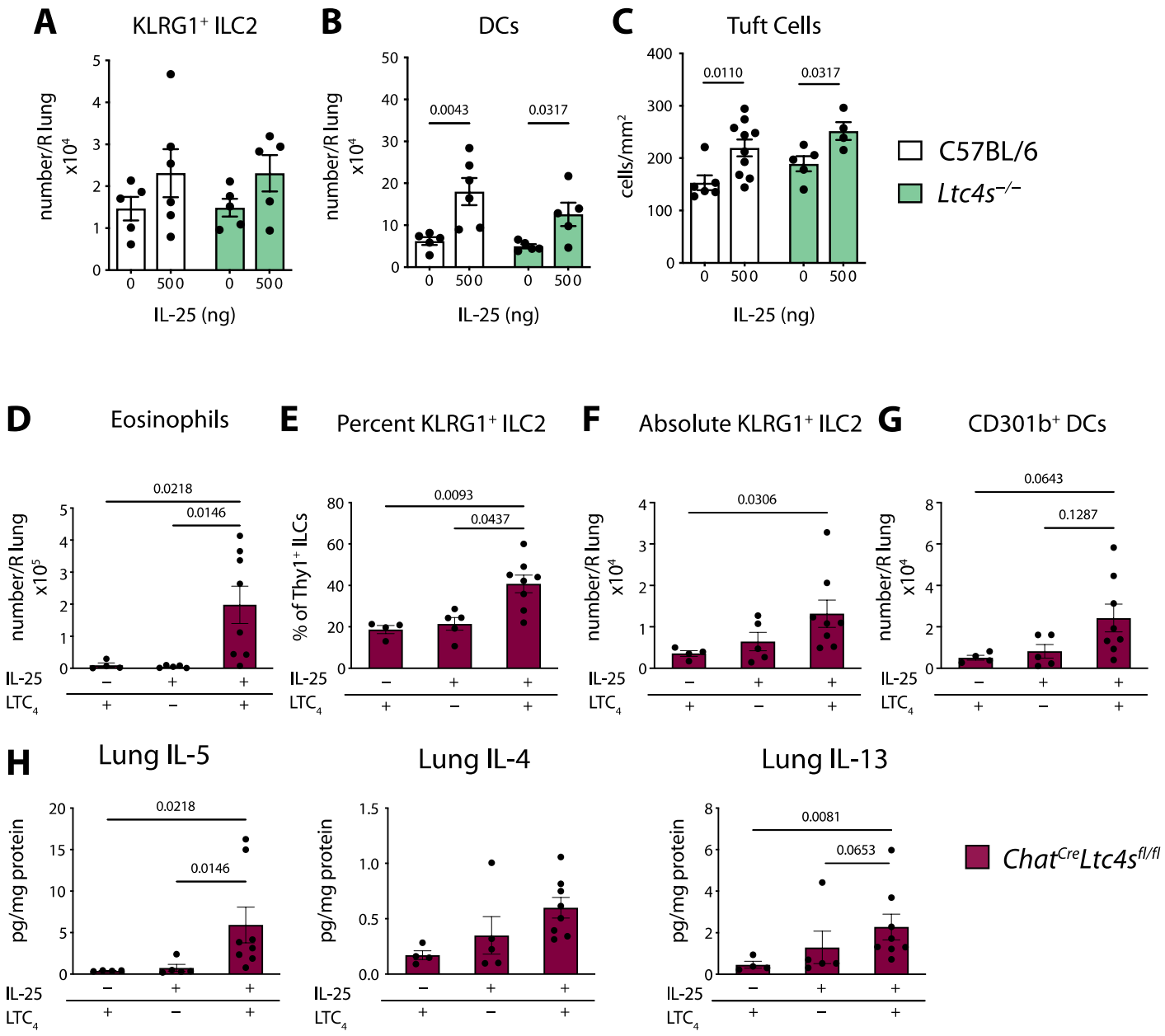
A
KLRG1+ ILC2
number/R lung x10^4
IL-25 (ng)
B
DCs
number/R lung x10^4
0.0043
0.0317
IL-25 (ng)
C
Tuft Cells
cells/mm^2
0.0110
0.0317
IL-25 (ng)
C57BL/6
Ltc4s−/−
D
Eosinophils
number/R lung x10^5
0.0218
0.0146
E
Percent KLRG1+ ILC2
% of Thy1+ ILCs
0.0093
0.0437
F
Absolute KLRG1+ ILC2
number/R lung x10^4
0.0306
G
CD301b+ DCs
number/R lung x10^4
0.0643
0.1287
IL-25
LTC4
H
Lung IL-5
pg/mg protein
0.0218
0.0146
Lung IL-4
pg/mg protein
Lung IL-13
pg/mg protein
0.0081
0.0653
ChatCreLtc4sfl/fl

Fig. S8. *Ltc4s* deletion does not alter the airway responses to IL-25. (**A**) WT and *Ltc4s*$^{-/-}$ mice were given 3 daily intranasal doses of 500 ng of IL-25 and assessed 2 days after the last dose (**Fig. 1A** schema). (**A, B**) Lung KLRG1^{+} ILC2 numbers (**A**) and DCs (**B**) were assessed by FACS. (**C**) DCLK1^{+} tuft cells were enumerated in the trachea. (**D-G**) *Chat*^{Cre}*Ltc4s*$^{fl/fl}$ mice were given LTC_4 (1.6 nmol), or IL-25 (100 ng) or a combination of LTC_4 and IL-25 and assessed 2 days after the last dose (**Fig. 1A** schema). (**D**) The number of eosinophils, (**E, F**) frequency and number of KLRG1^{+}ICOS^{+}Thy1.2^{+} ILC2s and (**G**) number of CD301b^{+} DCs in the lung were assessed by FACS. (**H**) Lung cytokine protein concentration was determined by LegendPlex in lung homogenates. Data are means ± SEM pooled from 2 or 3 independent experiments, each dot is a separate mouse, p values <0.05 indicated, Kruskal-Wallis ANOVA with Dunn's correction for multiple comparisons.

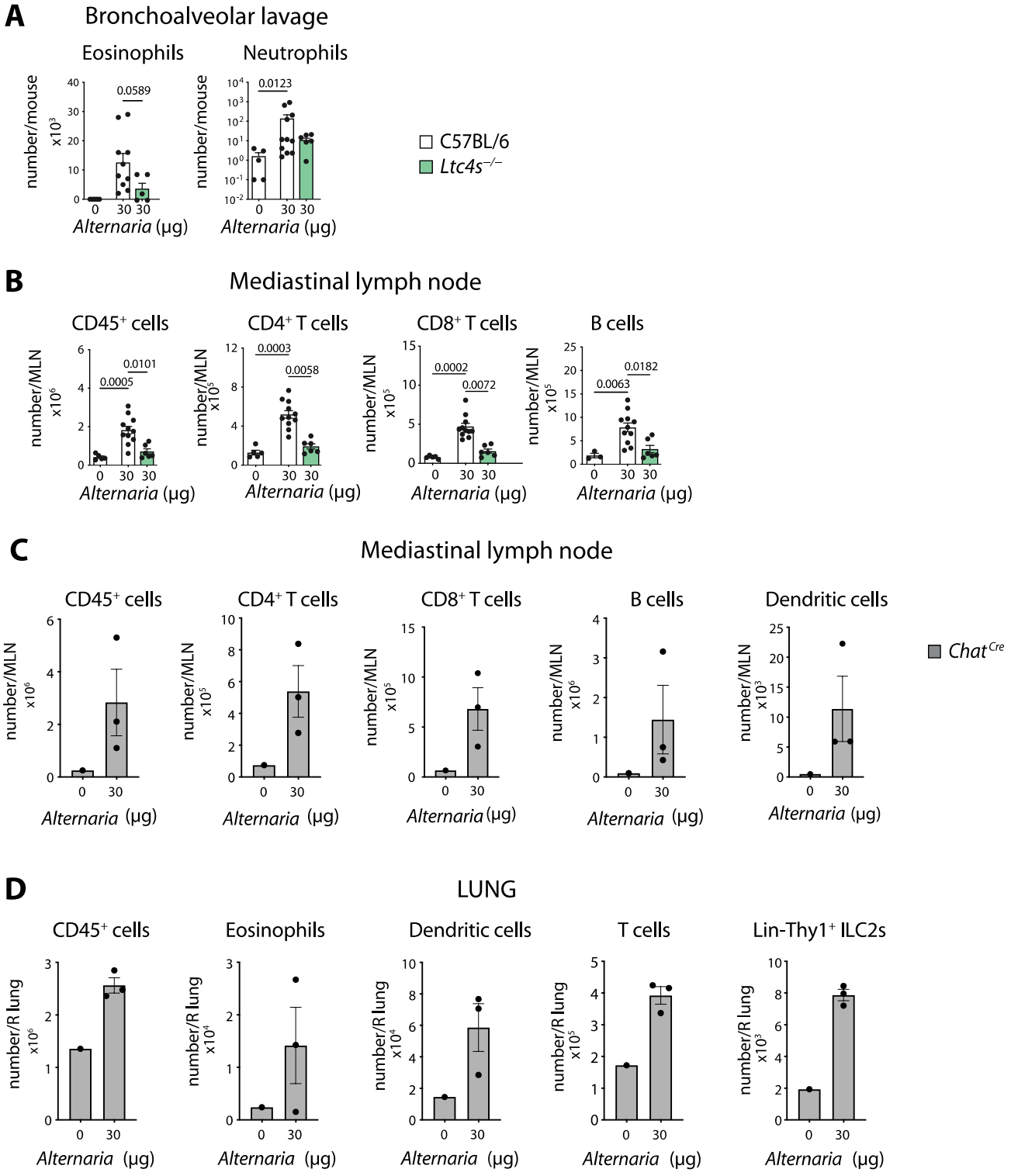
A
Bronchoalveolar lavage
Eosinophils
Neutrophils
number/mouse
x10³
0.0589
0.0123
0 30 30
Alternaria (μg)
C57BL/6
Ltc4s−/−
B
Mediastinal lymph node
CD45⁺ cells
CD4⁺ T cells
CD8⁺ T cells
B cells
number/MLN
x10⁶
x10⁵
0.0005
0.0101
0.0003
0.0058
0.0002
0.0072
0.0063
0.0182
C
Mediastinal lymph node
CD45⁺ cells
CD4⁺ T cells
CD8⁺ T cells
B cells
Dendritic cells
number/MLN
x10⁶
x10⁵
x10³
0 30
Alternaria (μg)
Chat Cre
D
LUNG
CD45⁺ cells
Eosinophils
Dendritic cells
T cells
Lin-Thy1⁺ ILC2s
number/R lung
x10⁶
x10⁴
x10⁵
x10³
0 30
Alternaria (μg)

Fig. S9. Lung and lymph node responses to *Alternaria* in *Ltc4s*$^{-/-}$ and *Chat*^{Cre} mice .

(A-B) C57BL/6 and *Ltc4s*$^{-/-}$ mice were given a single intranasal dose of *Alternaria* and were evaluated 24 hours after the challenge. (**A**) Bronchoalveolar lavage cells were counted, and eosinophils and neutrophils were evaluated using Diff-Quick stain. (**B**) Mediastinal lymph node (MLN) numbers of CD45$^+$ cells, CD4$^+$ and CD8$^+$ T cells and B cells were evaluated by FACS. Data are means ± SEM pooled from ≥ 2 independent experiments, each dot is a separate mouse, p values from Mann Whitney t test are indicated. **(C-D)** *Chat*^{Cre} mice were given a single intranasal dose of *Alternaria* and were evaluated 48 hours later. (**C**) Mediastinal lymph node (MLN) numbers of CD45$^+$ cells, CD4$^+$ and CD8$^+$ T cells and B cells were evaluated by FACS. **(D)** Lung CD45$^+$ cells, eosinophils, DCs, T cells and Thy1$^+$ILC2s were assessed by FACS.